

## Astrocyte $\text{Ca}^{2+}$ waves trigger responses in microglial cells in brain slices

Carola G. Schipke\*, Clemens Boucsein\*, Carsten Ohlemeyer\*, Frank Kirchhoff†, and Helmut Kettenmann\*

Max-Delbrück Center for Molecular Medicine, Cellular Neuroscience, Robert-Rössle-Straße 10, D-13092 Berlin, Germany; and †Max Planck Institute of Experimental Medicine, Neurogenetics, Hermann-Rein-Str. 3, D-37075 Göttingen, Germany

Corresponding author: Cellular Neuroscience, Max Delbrück Center for Molecular Medicine, Robert-Rössle-Strasse 10, D-13092 Berlin, Germany. E-mail: hketten@mdc-berlin.de

### ABSTRACT

Pathologic impacts in the brain lead to a widespread activation of microglial cells far beyond the site of injury. Here, we demonstrate that glial  $\text{Ca}^{2+}$  waves can trigger responses in microglial cells. We elicited  $\text{Ca}^{2+}$  waves in corpus callosum glial cells by electrical stimulation or local adenosine triphosphate (ATP) ejection in acute brain slices. Macroglial cells, but not microglia, were bulk-loaded with  $\text{Ca}^{2+}$ -sensitive dyes. Using a transgenic animal in which astrocytes were labeled by the enhanced green fluorescence protein (EGFP) allowed us to identify the reacting cell populations: the wave activated a  $\text{Ca}^{2+}$  response in both astrocytes and non-astrocytic glial cells and spread over hundreds of micrometers even into the adjacent cortical and ventricular cell layers. Regenerative ATP release and subsequent activation of metabotropic purinergic receptors caused the propagation of the glial  $\text{Ca}^{2+}$  wave: the wave was blocked by the purinergic receptor antagonist Reactive Blue 2 and was not affected by the gap junction blocker octanol, but enhanced in  $\text{Ca}^{2+}$  free saline. To test whether microglial cells respond to the wave, microglial cells were labeled with a dye-coupled lectin and membrane currents were recorded with the patch-clamp technique. When the wave passed by, a current with the characteristics of a purinergic response was activated. Thus,  $\text{Ca}^{2+}$  waves *in situ* are not restricted to astrocytic cells, but broadly activate different glial cell types.

Key words: mouse • astrocyte • ATP-release • calcium-wave • microglia • brain slice

**F**or a long time, glial cells in general have been considered passive elements in the brain but are now regarded as elements that sense and respond to neuronal activity (1). In particular, astrocytes express a large variety of transmitter and hormone receptors as sensors for synaptic activity and, furthermore, can communicate over long distances, namely via waves of intracellular  $\text{Ca}^{2+}$  elevation (2, 3). These  $\text{Ca}^{2+}$  waves travel within the astrocytic cell populations and have been characterized in primary cultures, slice cultures, and in the isolated retina (2, 4–6). Two different mechanisms have been described to explain how the  $\text{Ca}^{2+}$ -wave propagates within an astrocytic network in culture: A) the diffusion of second messengers via gap junctions between highly coupled astrocytes with subsequent  $\text{Ca}^{2+}$ -release from intracellular stores (6) or B) the release of the transmitter adenosine triphosphate (ATP) from astrocytes into the

extracellular space followed by purinergic receptor activation on neighboring cells, which, in turn, leads to elevation of internal calcium (7, 8). Few experiments have been carried out so far on astrocytic  $\text{Ca}^{2+}$  wave propagations in living, acutely isolated brain tissue. Newman and Zahs (9) established that an astrocytic  $\text{Ca}^{2+}$  wave can propagate within the intact retina, and they showed that the wave recruits Müller cells, a radial glial cell with some astrocyte features. In this preparation, the wave spreads via ATP release and concomitant purinergic receptor activation (4). The mechanisms leading to ATP release are yet unknown. ATP release seems to be  $\text{Ca}^{2+}$  independent (7), whereas the release of glutamate depends on increased cytosolic  $\text{Ca}^{2+}$  levels (10, 11). Toxins that interfere with the SNARE-complex block the glutamate release, a finding that suggests a vesicular release mechanism comparable with synaptic exocytosis (12). Consequently, intracellular calcium changes in astrocytes can influence neuronal activity (13–15).

Although astrocytic calcium waves are discussed mostly as a mean by which astrocytes influence neuronal signal transmission, they would also meet the requirements for a mechanism signaling pathological events in the brain over large distances. There is evidence that glial cells can sense pathologic events, which have occurred hundreds of micrometers away. After brain injury, microglial cells are activated several millimeters away from the lesion site (16, 17). Microglial cells are the major immunocompetent element of the central nervous system (CNS) and react with a complex and graded response to any type of CNS injury (18). The initial signal that triggers microglial activation is still unknown. Cultured cells show an activated phenotype after challenge with various pathology-related substances, such as bacterial cell wall components (19) and complement fragments (20), but also after incubation with ATP (21). Thus, ATP is a candidate for signaling injury to microglia, because these cells, at least in culture, express several subtypes of purinergic receptors (22). Stimulation of microglial purinergic receptors in culture leads to the release of tumor necrosis factor  $\alpha$  (TNF- $\alpha$ ) and modulation of interleukin (IL)-1beta release (21, 23).

In the present study, we have found conditions to trigger  $\text{Ca}^{2+}$  waves in acute slices of brain tissue, and we have shown that the wave, carried by sequential ATP-release, leads to a global response in glia, including microglial cells.

## **MATERIALS AND METHODS**

### **Animals, preparation of brain slices, and calcium recordings**

For slice preparation, 5- to 8-day old mice (either glial fibrillary acidic protein (GFAP)/EGFP transgenic FVB/N mice (17) or nontransgenic NMRI mice) were decapitated and their brains were removed. Frontal slices of 250–300  $\mu\text{m}$  thickness were cut using a vibratome (Vibracut, FTB Feinwerktechnik, Bensheim, Germany) in ice-cold bicarbonate buffer. Slices were stored at room temperature in gassed buffer for at least 20 min before staining.

Slices were incubated with the  $\text{Ca}^{2+}$  indicator dyes Fluo-4-acetoxymethylester (10  $\mu\text{M}$  Fluo-4-AM, Molecular Probes, Eugene, OR) or Calcium Orange-acetoxymethylester (10  $\mu\text{M}$  Calcium Orange-AM, Molecular Probes) in bicarbonate buffer at 37°C and 5%  $\text{CO}_2$  for 40 to 60 min or at room temperature for 90–120 min. Slices were transferred to a perfusion chamber on an upright microscope (Axioskop FS, Zeiss, Oberkochen, Germany) and fixed in the chamber by using a U-shaped platinum wire with a grid of nylon threads. Slices were superfused with gassed

bicarbonate buffer at a flow rate of 4 to 6 ml/min. Substances were applied by changing the perfusate. Intracellular  $\text{Ca}^{2+}$  changes were detected by using either a confocal laser scanning microscope (Sarastro 2000, Molecular Dynamics, Sunnyvale, CA) or a cooled CCD camera (SensiCam, PCO, Kelheim, Germany). We used the 488 nm band of an Ar+/Kr+-laser or a monochromator set to 488 nm (Till Photonics, München, Germany), respectively, as a light source for fluorophore excitation. Due to the scanning rate of the confocal microscope, the sampling rate was limited to 0.25 Hz, whereas with the CCD-camera 1 Hz was achieved. Images were stored on a PC and processed with conventional software (ImagePro, Media Cybernetics, Silver Spring, MD). For better illustrating the moving front of a  $\text{Ca}^{2+}$  wave, we subtracted from each image the pixel values of the previous image. This procedure results in a series of images, which highlights only those regions, that have changed from one image to the next and thus shows the newly responding cells. Electrical stimulation was accomplished with a conventional glass electrode filled with bath solution. The pipettes had a resistance of  $\sim 1$  Mohm, which corresponds to a tip opening of  $\sim 15$   $\mu\text{m}$ . The tip of the pipette was placed on top of the slice, with the pipette only gently touching the upper cell layer. After the positioning of the pipette the slice was allowed to recover from mechanical stress for at least 2 min. Chemical stimulation was performed by ejecting ATP-containing solution from a micropipette with a tip opening of  $\sim 5$   $\mu\text{m}$ . Before the induction of the wave, the slice was superfused with  $\text{Ca}^{2+}$  free solution for 2 min. Then, the bath perfusion was stopped. The wave was elicited by applying 10 Hz stimulation for 4 s. This stimulation paradigm was chosen as it induced solid responses. In some cases, however, shorter stimulation—even only a few pulses—was also effective in eliciting a wave. The  $\text{Ca}^{2+}$  wave could be triggered repetitively within the same area. Time between stimulations was at least 5 min, and slices were superfused with  $\text{Ca}^{2+}$  containing solution during recovery times.

### **Electrophysiological recordings**

We used the patch-clamp technique in the whole cell configuration for recording membrane currents. Electrodes with a resistance of 6–8 MOhm were pulled and filled with pipette solution. Because cell somata were located approximately 10–30  $\mu\text{m}$  underneath the slice surface, we applied pressure to the pipette while it was advanced towards the cell. Uncompensated currents were recorded with conventional electronics (EPC-7 or EPC9-amplifier, HEKA electronics, Lambrecht/Pfalz, Germany).

To identify microglial cells, slices were stained with Texas Red-coupled lectin from *Lycopersicon esculentum* (tomato lectin, Sigma, Deisenhofen, Germany). The lectin was added to the Fluo-4-AM containing bicarbonate buffer. Tomato lectin labeled the microglial cells while the slices were loaded with the  $\text{Ca}^{2+}$ -sensor for 45 min at 37°C in carbogen atmosphere (5%  $\text{CO}_2$ , 95%  $\text{O}_2$ ).

### **Solutions and electrodes**

The standard bath solution contained 134 mM NaCl, 2.5 mM KCl, 2 mM  $\text{CaCl}_2$ , 1.3 mM  $\text{MgCl}_2$ , 26 mM  $\text{NaHCO}_3$ , 1.25 mM  $\text{K}_2\text{HPO}_4$ , 10 mM glucose, and 2 mg/l phenol red as pH indicator. By gassing the solutions with carbogen, we could then adjust the pH to 7.4–7.5. The pipette solution for patch clamp recordings contained 130 mM KCl, 2 mM  $\text{MgCl}_2$ , 0.5 mM  $\text{CaCl}_2$ , 2 mM Na-ATP, 5 mM ethylene glycol-bis( $\beta$ -aminoethylether)-N,N,N',N'-tetraacetic acid (EGTA), 10 mM N-(2-hydroxyethyl) piperazine-2'-(2-ethanesulphonic acid) (HEPES).  $\text{Ca}^{2+}$  activity of the pipette solution was  $\sim 11$  nM. All experiments were carried out at room temperature. Recording and

stimulation pipettes were fabricated from borosilicate capillaries (Hilgenberg, Malsfeld, Germany). Drugs were applied to the bath solution in the following concentrations ( $\mu\text{M}$ ): Reactive Blue 2 (30), Suramin (100), 6-cyano-7-nitroquinoxaline-2,3-dione (CNQX) (50), octanol (500),  $\text{Cd}^{2+}$  (100), Tetrodotoxin (TTX) (1), ((+)-alpha-methyl-4-carboxy-phenylglycine) (MCPG) (50), thapsigargin (20).

## RESULTS

### **$\text{Ca}^{2+}$ waves can be triggered in acute brain slices**

To record  $\text{Ca}^{2+}$  signals from glial cells, we incubated brain slices of young (P5 – P8) mice with the  $\text{Ca}^{2+}$ -sensitive dye Fluo-4-AM (10  $\mu\text{M}$ ). To select for glial cells, we focused on the corpus callosum, because this structure, as a white matter tract, contains no neuronal cell bodies and thus all Fluo-4 labeled somata were glial. To elicit a  $\text{Ca}^{2+}$  wave, we placed a pipette with a tip diameter of about 15  $\mu\text{m}$  onto the surface of the slice and stimulated it electrically (4 sec. at 10 Hz). Already during the stimulation period, we recorded a  $\text{Ca}^{2+}$  increase in cells close (10–20  $\mu\text{m}$ ) to the stimulation pipette. With a delay, cells in increasing distance from the pipette responded and this event was reminiscent of a spreading wave. Measuring the onset of the  $\text{Ca}^{2+}$  response with respect to the distance of the cell indicated the speed by which the wave traveled, namely at  $13.9 \pm 1.8 \mu\text{m/s}$  ( $n=26$ ). In some cases, the wave spread slightly more rapidly in the orientation of the axonal tracts. The  $\text{Ca}^{2+}$  signal propagated to the border of our observation area, which indicated that the wave extended over a distance of at least half a millimeter. The  $\text{Ca}^{2+}$  response of a given cell lasted for about 1 min, except for cells located in the close vicinity of the stimulation pipette in which the  $\text{Ca}^{2+}$  increase lasted for about 2 min. The wave could be evoked up to four times within the same region, if the slice was allowed to recover for about 5 min between stimulations. Local ATP ejection from a patch pipette also evoked a  $\text{Ca}^{2+}$  wave with similar features (data not shown). Cellular depolarization by extracellular application of buffer with high potassium concentrations was not sufficient to elicit a wave: local ejection of elevated  $[\text{K}^+]$  (100 mM) from a patch pipette induced only a transient  $\text{Ca}^{2+}$  elevation restricted to the site of application (data not shown).

The phenomenon of the spreading  $\text{Ca}^{2+}$  wave was not confined to the corpus callosum: cells in the adjacent cortical layers also responded with an increase in  $\text{Ca}^{2+}$ . The wave spread with a similar velocity within the cortical layers compared with the corpus callosum ([Fig. 1](#)).

### **Intracellular calcium stores give rise to enhanced cytosolic $\text{Ca}^{2+}$ levels**

To test for the source of  $\text{Ca}^{2+}$ , we compared responses in  $\text{Ca}^{2+}$  containing and  $\text{Ca}^{2+}$  free solution. The wave spread even further and recruited more cells in  $\text{Ca}^{2+}$  free solution than in normal buffer, which suggests that  $\text{Ca}^{2+}$  influx from the extracellular space does not cause the cytosolic  $\text{Ca}^{2+}$  transient. We therefore performed most of our experiments in nominally  $\text{Ca}^{2+}$  free solution. Complete depletion of internal  $\text{Ca}^{2+}$  stores abolished the  $\text{Ca}^{2+}$  wave as could be shown by an experimental paradigm, which leads to a depletion of  $\text{Ca}^{2+}$  stores (24) in cultured astrocytes, namely the application of ATP in the presence of thapsigargin, a blocker of  $\text{Ca}^{2+}$  uptake into the endoplasmic stores. The first application of ATP triggers an intracellular  $\text{Ca}^{2+}$  increase, but the refilling of stores is prevented by thapsigargin, so that a second application no longer leads to a significant  $\text{Ca}^{2+}$  increase. After eliciting a  $\text{Ca}^{2+}$  wave, we applied this depletion protocol.

Subsequently, still in the presence of thapsigargin, electrical stimulation did not elicit a  $\text{Ca}^{2+}$  wave, but the signal was restricted to the close proximity of the stimulation pipette ( $n=3$ ) ([Fig. 2](#)).

### **Different cell types react with a $\text{Ca}^{2+}$ signal during wave propagation**

To identify the cells that participate in the wave, we made use of a transgenic animal in which astrocytes are labeled by the enhanced green fluorescent protein (EGFP) (17). We have used the red-shifted fluorescent  $\text{Ca}^{2+}$  sensor Calcium Orange, which allowed for imaging of EGFP fluorescence and intracellular  $\text{Ca}^{2+}$  simultaneously. As shown in [Figure 3A](#), the wave propagated both in EGFP positive as well as in EGFP negative cells, which indicated that both astrocytes and non-astrocytic cells participate in the wave. To characterize the responding cells further, we studied the membrane current pattern with the patch clamp technique after we established that the cells were part of the  $\text{Ca}^{2+}$  wave. We recorded two different current patterns in response to voltage steps in de- and hyperpolarizing direction ([Fig. 3B](#)): cells with a linear current-voltage curve exhibited passive membrane currents with no sign of voltage activation and without the typical tail currents of the oligodendrocytes: this is the current pattern typical for astrocytes (25). A second population of cells was characterized by the lack of inward rectifier currents, a prominent delayed rectifying outward current and small sodium inward currents. This current pattern is characteristic for glial precursor cells (26). Thus, the wave propagates within astrocytes and glial precursor cells. As can be seen in [Figure 1](#), the wave spreads from the corpus callosum also to the ventricular wall, most likely to ependymal cells. These cells also display a strong  $\text{Ca}^{2+}$  signal.

### **ATP released into the extracellular space is the carrier of the $\text{Ca}^{2+}$ wave**

The spread of the  $\text{Ca}^{2+}$  wave was influenced strongly by the bath perfusion: as can be seen in [Figure 4](#), the wave travels radial from the stimulation pipette if the bath perfusion is stopped. With a rapid perfusion, as used in most physiological recording configurations, the  $\text{Ca}^{2+}$  increase was restricted to cells close to the pipette. A slow flow of buffer led to wave propagation predominantly in the direction of the bath flow, indicating that a diffusible substance mediates the wave ([Fig. 4A](#)). In cultured astrocytes,  $\text{Ca}^{2+}$  signals spread either due to propagation via gap junctions or through release of glutamate or ATP and consecutive activation of glutamatergic or purinergic receptors (2, 6, 27). To test for the involvement of purinergic receptors, we compared the propagation of the  $\text{Ca}^{2+}$  wave in the presence and absence of Reactive Blue 2, an antagonist for purinergic receptors. When slices were incubated for 2 min with Reactive Blue 2 (30  $\mu\text{M}$ ), stimulation resulted only in a local  $\text{Ca}^{2+}$  increase in the close vicinity of the stimulation pipette ( $n=5$ ) compared with the control ([Fig. 4B](#)). A similar result was obtained with suramin (100  $\mu\text{M}$ ) ( $n=5$ ), another antagonist of purinergic receptors (data not shown). To exclude the involvement of glutamatergic receptor activation, we carried out stimulations in the presence of 50  $\mu\text{M}$  MCPG ( $n=6$ ) and 50  $\mu\text{M}$  CNQX ( $n=4$ ) in different sets of experiments. The presences of these blockers did not alter the wave (data not shown). In addition, we performed experiments in the presence of 100  $\mu\text{M}$  glutamate to desensitize all glutamate receptors. Even in the presence of glutamate in the bath, a wave could be elicited (data not shown) ( $n=3$ ).

To exclude that electrical activity of axons is involved in the propagation of the wave, we incubated slices with 1  $\mu\text{M}$  TTX and 100  $\mu\text{M}$   $\text{Cd}^{2+}$ , thus blocking the generation of action

potentials and synaptic release, respectively ( $n=4$ ). The  $\text{Ca}^{2+}$  wave was not affected, indicating that the wave spread independent of neuronal activity (Fig. 5A). To test for wave propagation via gap junctions, slices were incubated for 2 min with the gap junction blocker octanol (500  $\mu\text{M}$ ) ( $n=3$ ). In acute retina preparations, octanol has been shown to block gap junctional coupling between astrocytes (28). Wave propagation was not affected by that treatment (Fig. 5B).

### The $\text{Ca}^{2+}$ wave triggers a response in microglia

Because microglial cells do not accumulate the calcium dyes, we analyzed the potential participation of microglial in the  $\text{Ca}^{2+}$  wave with electrophysiological methods. The cells were identified by specific staining with tomato lectin (lectin from *lycopersicon esculentum*, coupled to Texas Red) (29), which does not interfere with the physiological properties of microglial cells (30). Double labeling with a  $\text{Ca}^{2+}$  sensor and tomato lectin confirmed that microglia did not take up the  $\text{Ca}^{2+}$  dye. We approached the tomato lectin-labeled cells with the patch pipette and recorded membrane currents while eliciting a  $\text{Ca}^{2+}$  wave by electrical stimulation 50-100  $\mu\text{m}$  away from the patch pipette. As shown in Figure 6, microglia showed the transient induction of an outwardly rectifying current when the  $\text{Ca}^{2+}$  wave passed the cell. Of the 13 microglia investigated, 5 responded with this type of current to a passing wave. The induced current corresponds to currents observed in cultured microglia after stimulation with ATP (22). This finding suggests that microglial cells can sense the activation of other glial cells and participate in the global glial activity represented by the  $\text{Ca}^{2+}$  wave.

## DISCUSSION

Glial cells lack the ability to generate action potentials and thus cannot communicate via propagating electrical activity. Yet the astrocytic form for transferring information within their cellular network is mediated by  $\text{Ca}^{2+}$  signaling.  $\text{Ca}^{2+}$  waves that have been described in astrocyte cultures and mechanisms underlying this form of glial cell communication are due to either propagation via gap junctions (5) or ATP release/activation of purinergic receptors (31). Waves of  $\text{Ca}^{2+}$  through astrocytic networks have been found in slice cultures (32) and in the isolated retina (4).

Our experiments demonstrate that such waves can be activated in brain tissue and can spread over hundreds of micrometers from their site of origin. This response is not restricted to astrocytes, but it spreads to microglia and glial progenitor cells, as identified by their current patterns in response to de- and hyperpolarizing voltage jumps (26, 30), and can thus be viewed as a global glial wave. Our data indicate that, as in the retina, the propagation of the  $\text{Ca}^{2+}$  wave is mediated by release of ATP and subsequent activation of purinergic receptors and involves  $\text{Ca}^{2+}$  release from cytoplasmic stores. Unlike in culture, gap junctions are not an essential prerequisite for the wave to propagate in our experiments. Expression of connexin 43, a gap junction protein subunit, in microglia has been shown four days after a stab wound lesion (33). In acute slices, however, we have not observed any dye-coupling between microglial or between microglia and any other cell type (30). Thus, gap junctional coupling is not a possible mechanism to signal to and from microglia in the unlesioned brain.

We assume that there is a propagation of ATP release; that is, that ATP is released from one cell and triggers the release of ATP from neighboring cells. We think that it is unlikely that ATP is



released only from the initially stimulated cells because the amount of ATP released from ~10 cells would not be sufficient to trigger large  $\text{Ca}^{2+}$  responses in cells located 250  $\mu\text{M}$  away. The amplitude of the microglial response hints to a local concentration ~100  $\mu\text{M}$  ATP, because the response can be mimicked with this concentration (unpublished results). Moreover, the initial trigger does not destroy the cells in the close vicinity of the stimulation pipette, as the wave can be initiated several times from the same group of cells. Our finding that the wave spreads better in the direction of the axonal pathways hints to the fact that ATP also spreads within the slice and not only along its surface.

The initial signal that communicates CNS injury to microglia is unknown. Astrocytic  $\text{Ca}^{2+}$  waves and concomitant ATP-release could communicate such an injury to uninjured areas and could lead to the activation of microglial cells via purinergic receptor activation. As a response to a focal ischemic lesion, for instance, widespread microglial activation occurs, even in tissue that shows no sign of damage (16). Microglial cells are even activated during spreading depression (34). Purinergic receptors are expressed prominently by microglial cells (35, 22), and stimulation of purinergic receptors in cultured microglia leads to release of  $\text{TNF-}\alpha$  and modulation of IL-1 $\beta$  release, two cytokines well established to be involved in pathologic cascades.(21, 23, 36). It has been shown that cytokines themselves can influence ATP release from astrocytes (37) and thereby influence wave propagation (38). Moreover, essentially all types of glial cells, namely astrocytes (39), oligodendrocytes and their progenitors (40), and microglial cells (22) express various types of purinoreceptors and this receptor family can be viewed as the backbone of a common glial communication system.

## ACKNOWLEDGMENT

This work was supported by Deutsche Forschungsgemeinschaft (grant SFB 515 and Schwerpunktprogramm “Microglia” to H. K.).

## REFERENCES

1. Araque, A., Parpura, V., Sanzgiri, R. P., and Haydon, P. G. (1999) Tripartite synapses: glia, the unacknowledged partner. *Trends Neurosci.* **22**, 208–215
2. Cornell-Bell, A. H., Finkbeiner, S. M., Cooper, M. S., and Smith, S. J. (1990) Glutamate induces calcium waves in cultured astrocytes: long-range glial signaling. *Science* **247**, 470–473
3. Charles, A. C., Merrill, J. E., Dirksen, E. R., and Sanderson, M. J. (1991) Intercellular signaling in glial cells: calcium waves and oscillations in response to mechanical stimulation and glutamate. *Neuron* **6**, 983–992
4. Newman, E. A. (2001) Propagation of intercellular calcium waves in retinal astrocytes and Muller cells. *J. Neurosci.* **21**, 2215–2223
5. Giaume, C. and Venance, L. (1998) Intercellular calcium signaling and gap junctional communication in astrocytes. *Glia* **24**, 50–64

6. Venance, L., Premont, J., Glowinski, J., and Giaume, C. (1998) Gap junctional communication and pharmacological heterogeneity in astrocytes cultured from the rat striatum. *J. Physiol* **510** (Pt 2), 429–440
7. Wang, Z., Haydon, P. G., and Yeung, E. S. (2000) Direct observation of calcium-independent intercellular ATP signaling in astrocytes. *Anal. Chem.* **72**, 2001–2007
8. Cotrina, M. L., Lin, J. H., Lopez-Garcia, J. C., Naus, C. C., and Nedergaard, M. (2000) ATP-mediated glia signaling. *J. Neurosci.* **20**, 2835–2844
9. Newman, E. A. and Zahs, K. R. (1997) Calcium waves in retinal glial cells. *Science* **275**, 844–847
10. Bezzi, P., Carmignoto, G., Pasti, L., Vesce, S., Rossi, D., Rizzini, B. L., Pozzan, T., and Volterra, A. (1998) Prostaglandins stimulate calcium-dependent glutamate release in astrocytes. *Nature (London)* **391**, 281–285
11. Pasti, L., Zonta, M., Pozzan, T., Vicini, S., and Carmignoto, G. (2001) Cytosolic calcium oscillations in astrocytes may regulate exocytotic release of glutamate. *J. Neurosci.* **21**, 477–484
12. Araque, A., Li, N., Doyle, R. T., and Haydon, P. G. (2000) SNARE protein-dependent glutamate release from astrocytes. *J. Neurosci.* **20**, 666–673
13. Newman, E. A. and Zahs, K. R. (1998) Modulation of neuronal activity by glial cells in the retina. *J. Neurosci.* **18**, 4022–4028
14. Parpura, V. and Haydon, P. G. (2000) Physiological astrocytic calcium levels stimulate glutamate release to modulate adjacent neurons. *Proc. Natl. Acad. Sci. USA* **97**, 8629–8634
15. Hassinger, T. D., Atkinson, P. B., Strecker, G. J., Whalen, L. R., Dudek, F. E., Kossel, A. H., and Kater, S. B. (1995) Evidence for glutamate-mediated activation of hippocampal neurons by glial calcium waves. *J. Neurobiol.* **28**, 159–170
16. Lehrmann, E., Christensen, T., Zimmer, J., Diemer, N. H., and Finsen, B. (1997) Microglial and macrophage reactions mark progressive changes and define the penumbra in the rat neocortex and striatum after transient middle cerebral artery occlusion. *J. Comp. Neurol.* **386**, 461–476
17. Nolte, C., Matyash, M., Pivneva, T., Schipke, C. G., Ohlemeyer, C., Hanisch, U. K., Kirchhoff, F., and Kettenmann, H. (2001) GFAP promoter-controlled EGFP-expressing transgenic mice: a tool to visualize astrocytes and astrogliosis in living brain tissue. *Glia* **33**, 72–86
18. Kreutzberg, G. W. (1996) Microglia: a sensor for pathological events in the CNS. *Trends Neurosci.* **19**, 312–318

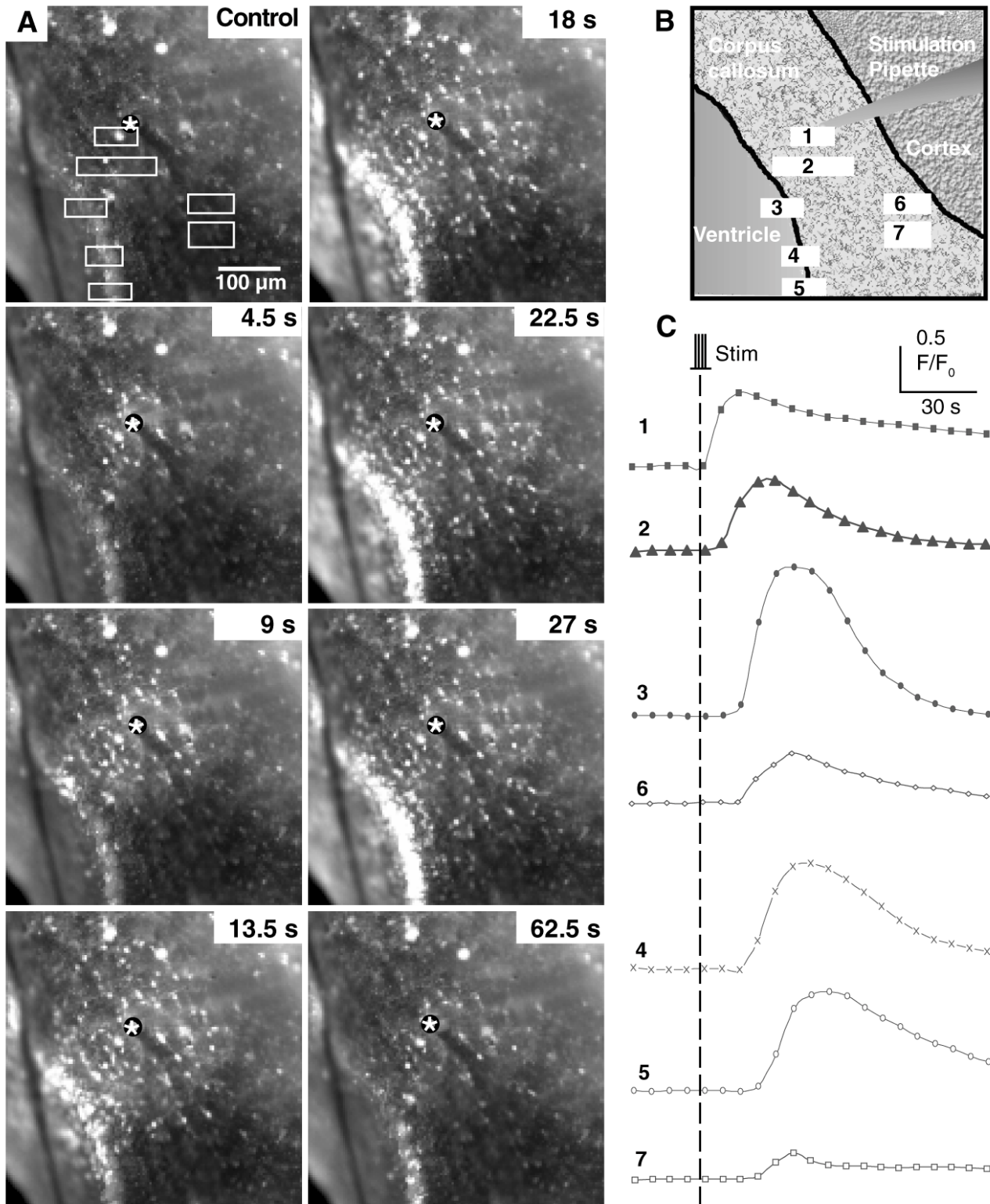


19. Prinz, M., Kann, O., Draheim, H. J., Schumann, R. R., Kettenmann, H., Weber, J. R., and Hanisch, U. K. (1999) Microglial activation by components of gram-positive and -negative bacteria: distinct and common routes to the induction of ion channels and cytokines. *J. Neuropathol. Exp. Neurol.* **58**, 1078–1089
20. Ilschner, S., Nolte, C., and Kettenmann, H. (1996) Complement factor C5a and epidermal growth factor trigger the activation of outward potassium currents in cultured murine microglia. *Neuroscience* **73**, 1109–1120
21. Hide, I., Tanaka, M., Inoue, A., Nakajima, K., Kohsaka, S., Inoue, K., and Nakata, Y. (2000) Extracellular ATP triggers tumor necrosis factor- $\alpha$  release from rat microglia. *J. Neurochem.* **75**, 965–972
22. Walz, W., Ilschner, S., Ohlemeyer, C., Banati, R., and Kettenmann, H. (1993) Extracellular ATP activates a cation conductance and a K<sup>+</sup> conductance in cultured microglial cells from mouse brain. *J. Neurosci.* **13**, 4403–4411
23. Ferrari, D., Chiozzi, P., Falzoni, S., Hanau, S., and Di Virgilio, F. (1997) Purinergic modulation of interleukin-1 beta release from microglial cells stimulated with bacterial endotoxin. *J. Exp. Med.* **185**, 579–582
24. Lytton, J., Westlin, M., and Hanley, M. R. (1991) Thapsigargin inhibits the sarcoplasmic or endoplasmic reticulum Ca-ATPase family of calcium pumps. *J. Biol. Chem.* **266**, 17067–17071
25. Chvatal, A., Pastor, A., Mauch, M., Sykova, E., and Kettenmann, H. (1995) Distinct populations of identified glial cells in the developing rat spinal cord slice: ion channel properties and cell morphology. *Eur. J. Neurosci.* **7**, 129–142
26. Berger, T., Schnitzer, J., and Kettenmann, H. (1991) Developmental changes in the membrane current pattern, K<sup>+</sup> buffer capacity, and morphology of glial cells in the corpus callosum slice. *J. Neurosci.* **11**, 3008–3024
27. Guthrie, P. B., Knappenberger, J., Segal, M., Bennett, M.V.L., Charles, A. C., and Kater, S. B. (1999) ATP released from astrocytes mediates glial calcium waves. *J. Neurosci.* **19**, 520–528
28. Zahs, K. R. and Newman, E. A. (1997) Asymmetric gap junctional coupling between glial cells in the rat retina. *Glia* **20**, 10–22
29. Acarin, L., Vela, J. M., Gonzalez, B., and Castellano, B. (1994) Demonstration of poly-N-acetyl lactosamine residues in amoeboid and ramified microglial cells in rat brain by tomato lectin binding. *J. Histochem. Cytochem.* **42**, 1033–1041
30. Boucsein, C., Kettenmann, H., and Nolte, C. (2000) Electrophysiological properties of microglial cells in normal and pathologic rat brain slices. *Eur. J. Neurosci.* **12**, 2049–2058

31. Fam, S. R., Gallagher, C. J., Salter, M. W. (2000) P2Y(1) purinoceptor-mediated Ca(2+) signaling and Ca(2+) wave propagation in dorsal spinal cord astrocytes. *J. Neurosci.* **20**, 2800–2808
32. Dani, J. W., Chernjavsky, A., and Smith, S. J. (1992) Neuronal activity triggers calcium waves in hippocampal astrocyte networks. *Neuron* **8**, 429–440
33. Eugenin, E. A., Eckardt, D., Theis, M., Willecke, K., Bennett, M. V., and Saez, J. C. (2001) Microglia at brain stab wounds express connexin 43 and in vitro form functional gap junctions after treatment with interferon-gamma and tumor necrosis factor-alpha. *Proc. Natl. Acad. Sci. USA* **98**, 4190–4195
34. Gehrman, J., Mies, G., Bonnekoh, P., Banati, R., Iijima, T., Kreutzberg, G. W., and Hossmann, K. A. (1993) Microglial reaction in the rat cerebral cortex induced by cortical spreading depression. *Brain Pathol.* **3**, 11–17
35. Norenberg, W., Cordes, A., Blohbaum, G., Frohlich, R., and Illes, P. (1997) Coexistence of purino- and pyrimidinoceptors on activated rat microglial cells. *Br. J. Pharmacol.* **121**, 1087–1098
36. Ferrari, D., Chiozzi, P., Falzoni, S., Dal Susino, M., Collo, G., Buell, G., Di Virgilio, and F. (1997) ATP-mediated cytotoxicity in microglial cells. *Neuropharmacology* **36**, 1295–1301
37. Verderio, C. and Matteoli, M. (2001) Atp mediates calcium signaling between astrocytes and microglial cells: modulation by ifn-gamma. *J. Immunol.* **166**, 6383–6391
38. John, G. R., Scemes, E., Suadicani, S. O., Liu, J. S., Charles, P. C., Lee, S. C., Spray, D. C., and Brosnan, C. F. (1999) IL-1beta differentially regulates calcium wave propagation between primary human fetal astrocytes via pathways involving P2 receptors and gap junction channels. *Proc. Natl. Acad. Sci. USA* **96**, 11613–11618
39. Walz, W., Gimpl, G., Ohlemeyer, C., and Kettenmann, H. (1994) Extracellular ATP-induced currents in astrocytes: involvement of a cation channel. *J. Neurosci. Res.* **38**, 12–18
40. Kirischuk, S., Scherer, J., Kettenmann, H., and Verkhratsky, A. (1995) Activation of P2-purinoreceptors triggered Ca<sup>2+</sup> release from InsP<sub>3</sub>-sensitive internal stores in mammalian oligodendrocytes. *J. Physiol. Lond.* **483**, 41–57

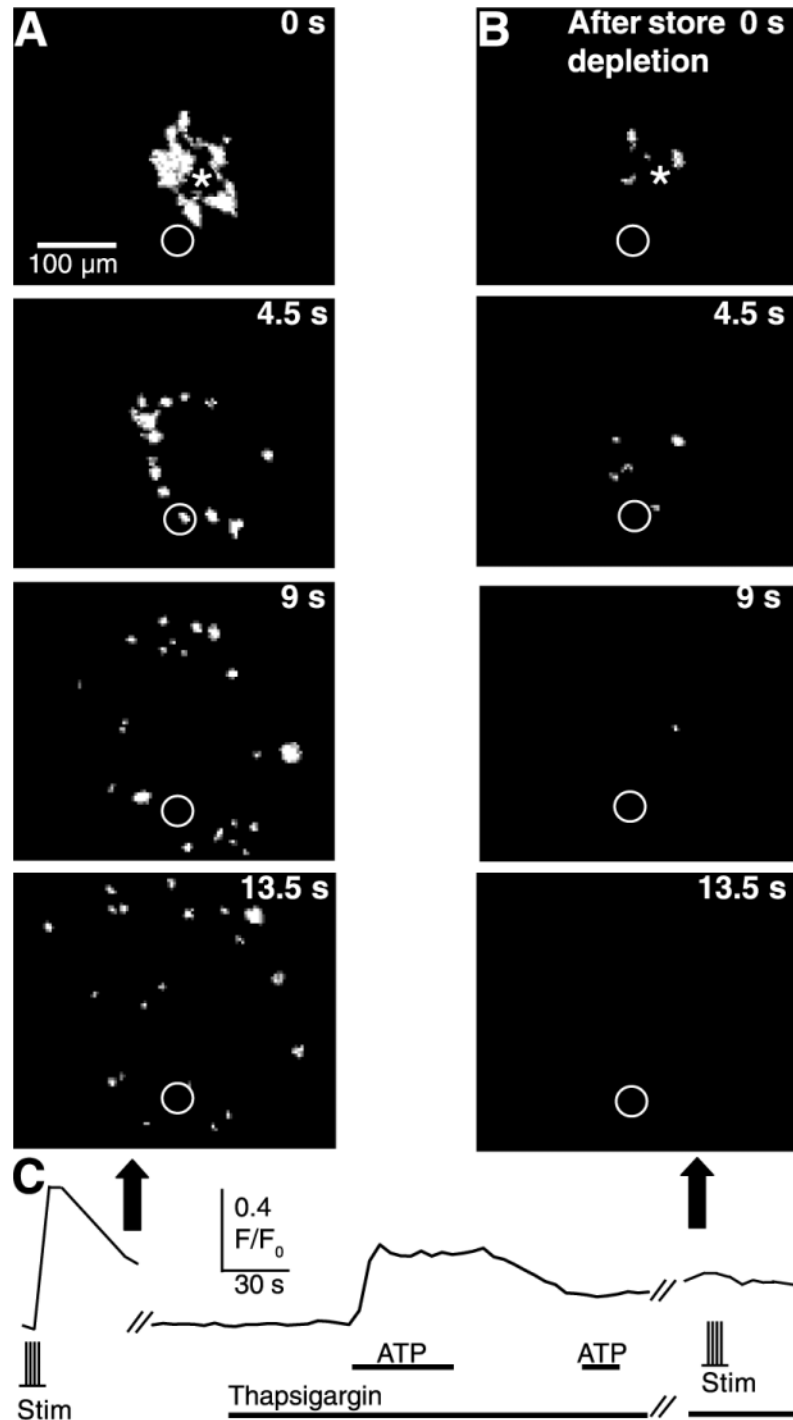
*Received August 21, 2001; revised November 8, 2001.*

Fig. 1



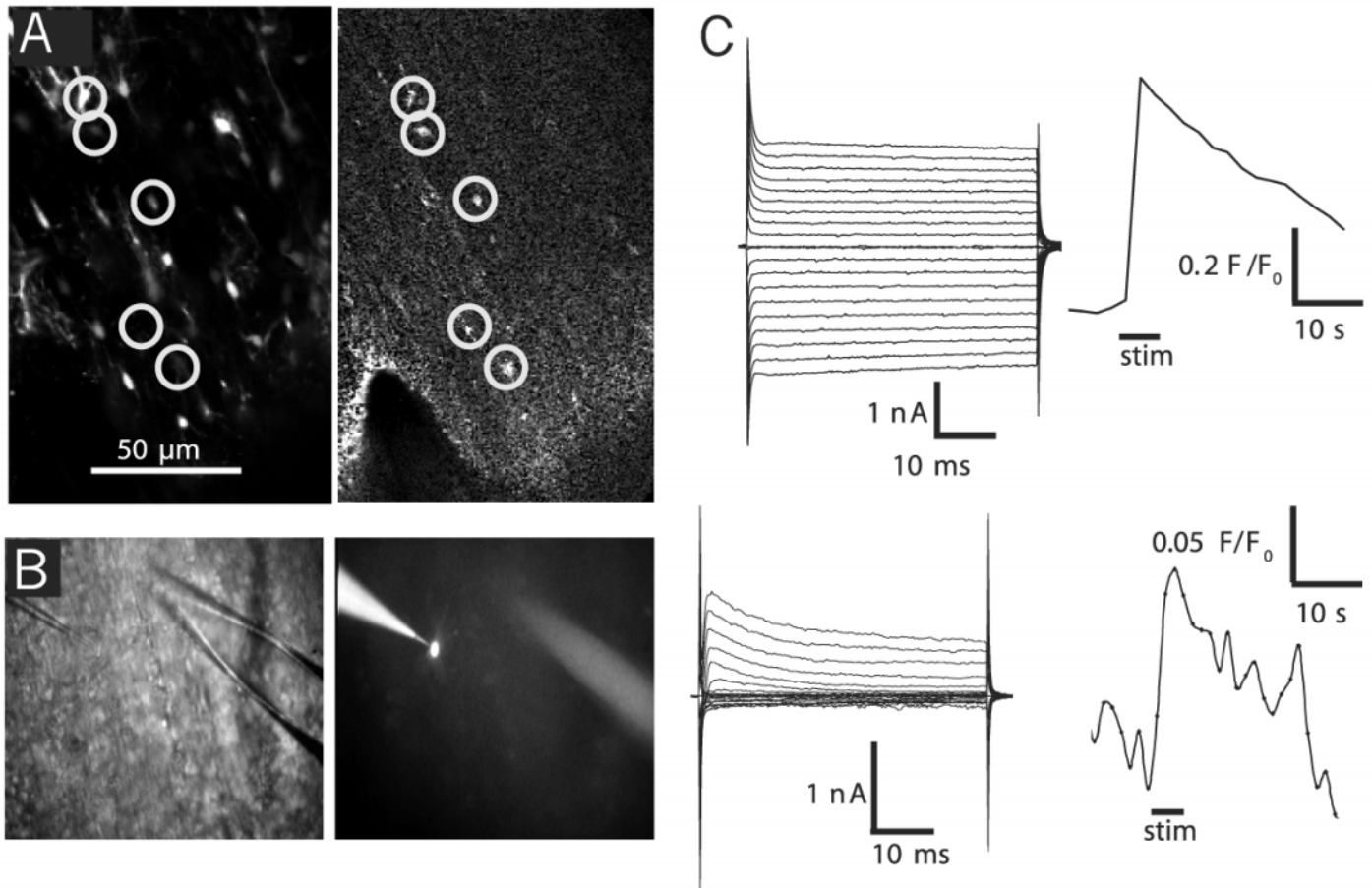
**Figure 1. Propagation of Ca<sup>2+</sup> waves in an acute brain slice.** A series of fluorescence images just before (control) and at defined times (as indicated) after electrical stimulation illustrate the spread of the Ca<sup>2+</sup> signal within a slice (A). The position of the stimulation electrode is marked by the asterisk. The cartoon in (B) outlines the anatomical structures of the fluorescence images. Moreover, the transient changes in Ca<sup>2+</sup> were measured at the indicated areas (B) and are displayed in (C). In area 1, close to the stimulation pipette, the increase in fluorescence (F/F<sub>0</sub>) occurred right after stimulation (indicated by a vertical line). At more distant areas, the delay amounted to several seconds. Note that cells in the ventricle wall respond with an intense signal.

Fig. 2



**Figure 2. The calcium signal is abolished after depletion of internal calcium stores. A)** A  $\text{Ca}^{2+}$  wave was elicited under control conditions. By subtracting consecutive images only the newly responding cells are displayed. The first image was recorded briefly after stimulation and subsequent ones with a delay as indicated. **B)** Internal calcium stores were depleted by application of thapsigargin ( $1 \mu\text{M}$ ), and two subsequent ATP applications still in the presence of thapsigargin. After this paradigm electrical stimulation did no longer trigger the induction of a  $\text{Ca}^{2+}$  wave as shown in the series of images in **(B)**. Calcium traces of the area outlined by the white circle in **(A)** and **(B)** are displayed in **(C)**. In addition, the responses to ATP and to thapsigargin are shown which is not illustrated in **(A)** or **(B)**.

**Fig. 3**



**Figure 3. Different cell populations participate in the  $\text{Ca}^{2+}$  wave.** **A)** To identify astrocytes, we obtained slices obtained from a transgenic animal in which astrocytes are labeled by the expression of the enhanced green fluorescent protein. The fluorescent micrograph on the left shows the intrinsic fluorescence of the EGFP-labeled astrocytes. On the right, the same area is displayed with filters for detection of Calcium Orange and thus for recording changes in intracellular  $\text{Ca}^{2+}$ . Electrical stimulation elicited a fluorescence increase in cells highlighted by circles. Note that not all of the responsive cells are astrocytes. **B)** After eliciting a  $\text{Ca}^{2+}$  wave, membrane currents were recorded from a responding cell. The micrograph on the upper left shows the arrangement of the recording (left) and stimulation pipette (right) as visualized with conventional optics. On the upper right, a fluorescence image for detecting Lucifer Yellow staining is displayed. Note the Lucifer Yellow filled cell and the recording pipette. **C)** The traces display currents activated in response to de- and hyperpolarizing voltage steps (from  $-160$  to  $+20$  mV, 10 mV increment) from a holding potential of  $-70$  mV. On the lower right, the fluorescence response ( $F/F_0$ ) of the  $\text{Ca}^{2+}$  dye Fluo-4 is displayed in response to stimulation. Current responses and fluorescence response of a different cell similar as described in **(B)**. Note the activation of outward currents with depolarization.

**Fig. 4**

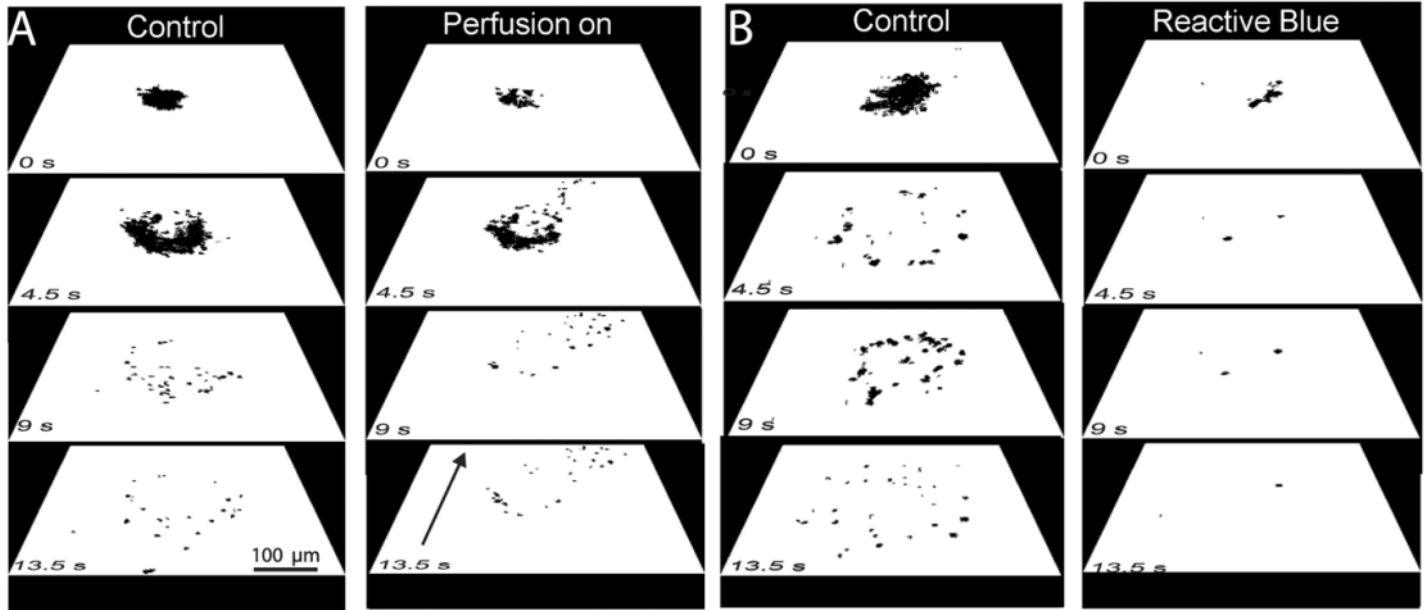


**Figure 4. Characteristics of the  $\text{Ca}^{2+}$  wave: effect of bath perfusion and Reactive Blue 2.** To illustrate the propagation of the  $\text{Ca}^{2+}$  wave, only those cells are displayed that were newly recruited to the population of  $\text{Ca}^{2+}$  responsive cells. This was achieved by subtracting the previous image from the one, which was displayed. The black areas represent the population of responsive cells at the times indicated. The first image shows the cells responding close to the pipette briefly after stimulation (0 s). In (A), two responses from the same field are shown, with no bath perfusion (left) and one with a slow perfusion into the direction of the arrow (right). In (B), a stimulation elicited a  $\text{Ca}^{2+}$  wave in control conditions (left), whereas only a local response was observed after applying the purinergic receptor antagonist Reactive Blue 2 (right).

**Fig. 5**

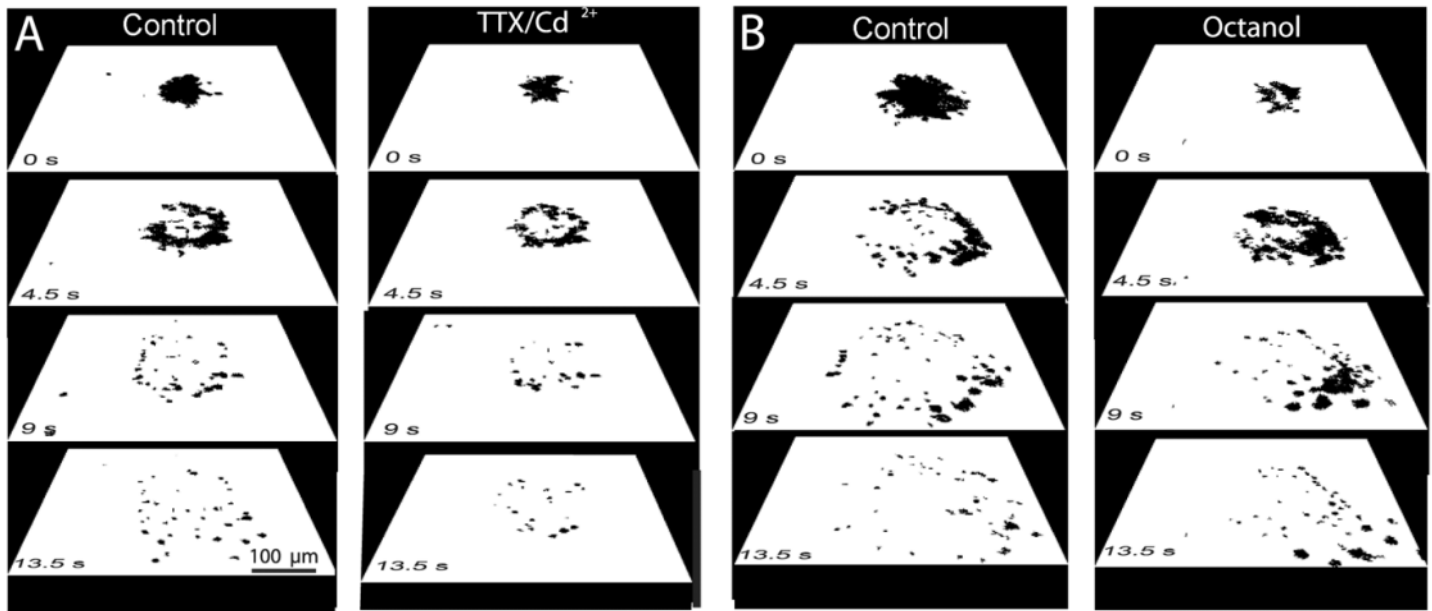


**Figure 5. The wave spreads independently from neuronal activity and does not propagate via gap junctions.** As in **Figure 4**, two responses from the same fields are shown. **A)** Stimulation elicited a Ca<sup>2+</sup> wave in control conditions (left), and the response was still present after superfusing the slice with 1 μM TTX and 100 μM Cd<sup>2+</sup> for 2 min before stimulating a second time (right). **B)** A stimulation-triggered response in control conditions (left) was compared to a response after the slice was superfused with 500 μM Octanol for 5 min. The spread of the wave was neither markedly affected by TTX/Cd<sup>2+</sup> nor by octanol.



Fig. 6

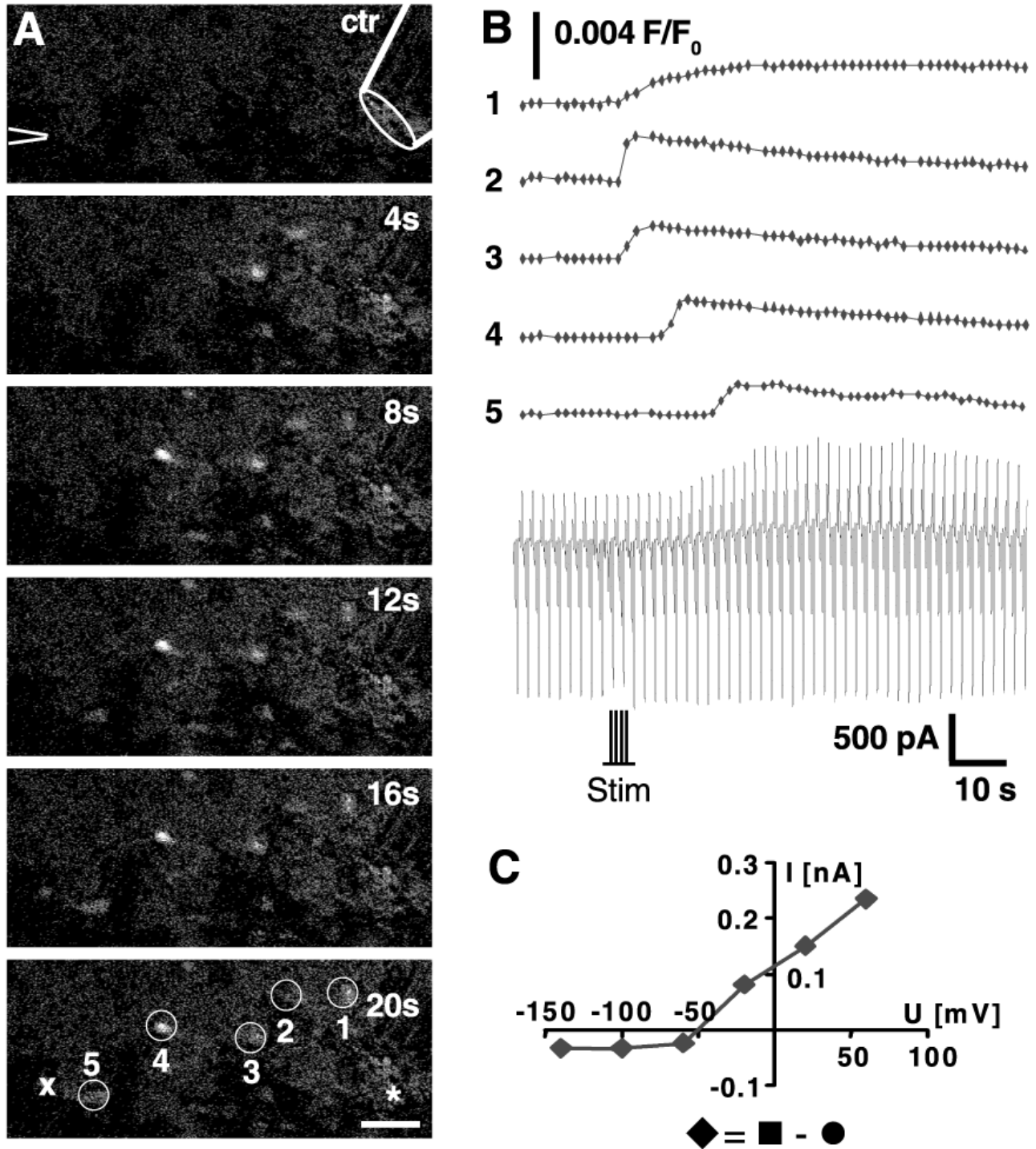


**Figure 6. Microglial cells sense and respond to the calcium wave.** The series of images in (A) illustrate the spread of a  $\text{Ca}^{2+}$  wave elicited by electrical stimulation. At the same time, membrane currents were recorded from a microglial cell. The position of the recording and stimulation pipette is indicated in the first image. The bar denotes  $20\ \mu\text{m}$  and the time after stimulation is indicated in each image recorded prior to stimulation (control). In (B), the transient changes in  $\text{Ca}^{2+}$  from five cells (indicated in the last image in A) are displayed in combination with the membrane currents recorded from the microglial cell. The membrane of the microglial cell was clamped at  $-20\ \text{mV}$ , and repetitively clamped to a series of de- and hyperpolarizing values. This procedure allowed us to construct current-to-voltage curves at 2-second intervals. It is evident that, with a delay in stimulation, outward currents increased in amplitude. In (C), the current voltage curve of the stimulation-induced current is displayed showing features of an outward rectifying  $\text{K}^+$  channel.